Chinese Journal of
POLYMER SCIENCE

RESEARCH ARTICEL

https://doi.org/10.1007/s10118-025-3338-2
Chinese J. Polym. Sci. **2025**, *43*, 1222–1230

Intrinsically Low Dielectric Constant and Low Dielectric Loss Polyimides Enabled by Rigid-Soft Structure

Hui Zhang[a], Hui-Shan Hu[a], Zhi-Yu Lu[a], Ming-Wei Liu[a], Hua Ge[a], Hui-Bo Yuan[a], Jian-Jun Song[b], Wan-Yi Tan[a*], Ting-Ting Cui[a*], and Yong-Gang Min[a*]

[a] *School of Materials and Energy, Guangdong University of Technology (GDUT), Guangzhou 510640, China*
[b] *Guangzhou Liangyue Materials Technology Co., Ltd., Guangzhou 510663, China*

Electronic Supplementary Information

Abstract Modified polyimides (MPIs) possess excellent thermal stability, chemical stability, and mechanical properties, and are considered to be a kind of dielectric material for high-frequency communication. Enhancing the rigidity of the polymer chains and intermolecular interactions can ensure low D_k/D_f at high frequency, which is attributed to the effective restriction of dipole orientations. However, it is difficult to achieve tight chain packing in an overly rigid polymer chain, whereas an overly flexible polymer chain might be insufficient to restrain small-scale molecular motions below T_g. To balance the trade-off between the rigidity of the polymer chains and tight chain packing, MPI was developed with a rigid-soft structure based on a naphthalene-alkyl-based diamine. On the one hand, incorporating the soft unit can enhance the movability of polymer chains to achieve dense chain packing for polyimides (PIs). On the other hand, the presence of rigid aromatic units can enhance intermolecular interactions and further restrict the motion of polar imide groups below T_g. As a result, the resultant MPI can prevent small-scale molecular motion below T_g. In contrast to the reference PI-TFMB-6FDA, D_k/D_f is significantly reduced from 2.72/0.0075 to 2.73/0.005 at a high frequency of 10 GHz. Furthermore, the rigid-soft structure endows PIs with good thermoplasticity owing to the good chain flexibility above T_g. In addition, PIs based on rigid-soft structures can preserve favorable thermal stability.

Keywords High-frequency communication; Polyimide; Dielectric loss

Citation: Zhang, H.; Hu, H. S.; Lu, Z. Y.; Liu, M. W.; Ge, H.; Yuan, H. B.; Song, J. J.; Tan, W. Y.; Cui, T. T.; Min, Y. G. Intrinsically low dielectric constant and low dielectric loss polyimides enabled by rigid-soft structure. *Chinese J. Polym. Sci.* **2025**, *43*, 1222–1230.

INTRODUCTION

With the rapid development of high-frequency communication technology, the demand for low-dielectric materials with a low dielectric constant (D_k) and low dielectric loss tangent (D_f) is increasing.[1−4] Modified polyimides (MPIs) possess excellent thermal stability, chemical stability, and mechanical properties and have been consistently used as dielectric materials for antenna materials.[5−8] As for MPIs, effective approaches for simultaneously lowering D_k and D_f include introducing porous structure[9−14] or fluoride groups,[15−20] decreasing the polarizability of polymers,[21−23] and increasing the rigidity of polymer chains[24−26] or their intermolecular interactions.[22,27−33] Fluorinated MPIs are always confronted with issues such as the high cost of fluorinated raw materials and the high complexity of their synthetic processes. Additionally, porous MPIs are likely to exhibit poor mechanical properties. Intrinsic MPIs with low polarizability are conducive to reducing D_k and D_f.[21−23] In general, the incorporation of a large amount of alkane structure can lead to a remarkable reduction in D_k and D_f, but it would result in poor thermal resistance.

The enhancement of the rigidity of the polymer chains and their intermolecular interactions can effectively restrain dipole orientations, thereby ensuring low D_k/D_f at high frequency, especially for D_f.[34−36] To date, there are several effective approaches for optimizing chain rigidity and intermolecular interactions, including adding additives[37−40] such as quasi-two-dimensional materials,[37] enhancing intermolecular interactions such as crosslinking[22,28,29,33,39] or other forces,[31,32] and introducing rigid units.[28,37] Li *et al.*[39] synthesized a series of phenylethynyl-terminated polyimide resins by grafting amine-functionalized hyperbranched polysiloxane (HBPSi). The incorporation of HBPSi led to a decreased dielectric constant, which was attributed to the increased free volume and low dielectric constant of silsesquioxane (Si—O—Si). Furthermore, the crosslinking and steric hindrance of HBPSi can effectively restrict the segmental mobility of PI chains, leading to a decreased dielectric loss tangent. Meng *et al.*[28] developed a new class of imide oligomers and

---

* Corresponding authors, E-mail: tanwanyi@gdut.edu.cn (W.Y.T.)
E-mail: cuitt@gdut.edu.cn (T.T.C.)
E-mail: ygmin@gdut.edu.cn (Y.G.M.)

Received January 18, 2025; Accepted March 12, 2025; Published online May 14, 2025

© Chinese Chemical Society
Institute of Chemistry, Chinese Academy of Sciences

thermosets using 9,9-bis(3,4-dicarboxyphenyl)fluorene dianhydride (BPAF). Through the cross-linking of phenyl-ethynyl groups, the BPAF-derived thermosets exhibited low D_f values of 0.0037 at high frequency from 30 GHz to 45 GHz and a low dielectric constant of 2.85, resulting from the stereochemical structure. In general, an overly rigid polymer chain is detrimental to tight chain packing, whereas an overly flexible polymer chain might be insufficient to restrain small-scale molecular motion below T_g. Neither of these issues is conducive to the dielectric properties. As the frequency is constantly increased, it is essential to conduct further research on dielectric materials, particularly for low-dielectric-loss materials, to meet the requirements of application in the field of high-frequency communication.

In the context, we develop “rigid-soft” structure to balance the trade-off between the rigidity of the polymer chain and tight chain packing based on a naphthalene-alkyl-based diamine. By regulating the ratio of soft to rigid units, the polymer chain can be maintained in close packing without significantly reducing the chain rigidity. As a result, the resultant structure can effectively restrain small-scale molecular motions below T_g, particularly the polar imide groups in PIs, thereby achieving low D_k/D_f. The relationship between “rigid-soft” structure and dielectric properties is studied in detail. Furthermore, it is found that MPIs with “rigid-soft” structure exhibit good chain flexibility above T_g and thereby good thermoplasticity.

EXPERIMENTAL

The materials sources and related characterizations are presented in the electronic supplementary information (ESI).

Synthesis and Characterization of MPIs

*Synthesis of 1,6-bis(4-bromophenoxy)hexane (Compound **1**)*

6-Bromonaphthalen-2-ol (13.43 g, 60.21 mmol) and potassium carbonate (16.68 g, 120.64 mmol) were added to *N*,*N*-dimethylformamide (DMF) (100 mL) and the mixture was stirred at 85 °C for 1 h. Then 1,6-dibromohexane (6.62 g, 27.13 mmol) was added and the mixture was stirred for another 12 h. After cooling to room temperature, the product was extracted using dichloromethane/deionized water. The product was further purified by column chromatography using dichloromethane/petroleum ether as the eluent and then recrystallized with ethanol overnight. Yield: 8.46 g (53.2%). ^{1}H-NMR (400 MHz, CDCl$_3$, δ):1.59–1.63 (m, 4H), 1.88–1.92 (m, 4H), 4.08 (t, 4H, J = 6.44 Hz), 7.09 (sd, 2H, J = 2.20 Hz), 7.17 (dd, 2H, J_1 = 8.92, J_2 = 2.44 Hz), 7.50 (dd, 2H, J_1 = 8.72, J_2 = 1.84 Hz), 7.58 (d, 2H, J = 8.76 Hz), 7.64 (d, 2H, J = 9.00 Hz), 7.90 (sd, 2H, J = 0.68 Hz).

Synthesis of 3,3'-((hexane-1,6-diylbis(oxy))bis(naphthalene-6,2-diyl))dianiline (DiHe-NaDA)

Compound **1** (8.46 g, 16.08 mmol), 3-aminophenylboronic acid (4.99 g, 36.47 mmol) and sodium carbonate (7.60 g, 71.70 mmol) were mixed in DMF (80 mL). Then, Pd(dppf)Cl$_2$ (0.38 g, 0.52 mmol) was added, and the reaction was stirred at 90 °C under N$_2$ for 12 h. After adding dichloromethane to extract the organic layer, the product was purified by column chromatography with dichloromethane/triethylamine as the eluent and recrystallized from ethyl acetate and alcohol, respectively. Yield: 5.23 g (58.9%). ^{1}H-NMR (400 MHz, DMSO-d$_6$, δ): 1.57 (m, 4H), 1.85 (m, 4H), 4.13 (t, 4H, J = 6.44 Hz), 5.25 (s, 4H), 6.59 (dd, 2H, J_1 = 8.08, J_2 = 2.16 Hz), 6.91 (d, 2H, J = 8.20 Hz), 6.96 (s, 2H), 7.13 (t, 2H, J = 7.80 Hz), 7.19 (dd, 2H, J_1 = 8.92, J_2 = 2.48 Hz), 7.33 (sd, 2H, J = 2.52 Hz), 7.69 (dd, 2H, J_1 = 8.48, J_2 = 1.84 Hz), 7.85 (d, 2H, J = 8.64 Hz), 7.88 (d, 2H, J = 9.04 Hz), 8.00 (s, 2H). MS (electrospray ionization) for [(M+H)$^+$, C$_{38}$H$_{37}$N$_2$O$_2$]: Calcd., 553.28, Found, 553.24.

Preparation of PI films

TFMB (3.48 g, 10.85 mmol) and 6FDA (4.82 g, 10.85 mmol) were added into DMAc (19.36 g), and stirred for 6 hours at room temperature. After defoaming under vacuum, the film was uniformly deposited on a clean glass substrate and heated at 200 °C for 30 min, 300 °C for 10 min, and 400 °C for 10 min for thermal imidization. After hot water immersion, the film was peeled off from the glass substrate, and the resulting PI film was named PI-TFMB-6FDA.

TFMB (3.30 g, 10.31 mmol) and DiHe-NaDA (0.30 g, 0.54 mmol) and 6FDA (4.82 g, 10.85 mmol) were added to DMAc (19.66 g). The other synthesis process was performed according to the above steps. This PI film was named as PI-DiHe-NaDA-5%.

TFMB (3.13 g, 9.77 mmol), DiHe-NaDA (0.60 g, 1.08 mmol) and 6FDA (4.82 g, 10.85 mmol) were added to DMAc (19.95 g). The other synthesis process was performed according to the above steps. This PI film was named as PI-DiHe-NaDA-10%.

TFMB (2.95 g, 9.23 mmol), DiHe-NaDA (0.90 g, 1.62 mmol) and 6FDA (4.82 g, 10.85 mmol) were added into DMAc (20.25 g). The other synthesis process was performed according to the above steps. This PI film was named as PI-DiHe-NaDA-15%.

RESULTS AND DISCUSSION

The synthetic route to naphthalene-alkyl-based diamine monomer 3,3'-((hexane-1,6-diylbis(oxy))bis(naphthalene-6,2-diyl))dianiline (DiHe-NaDA) is illustrated in Scheme 1. DiHe-NaDA was incorporated into PI-TFMB-6FDA to regulate the chain rigidity and packing characteristics. Copolymerized PIs were prepared with various ratios of DiHe-NaDA. FTIR spectroscopy revealed that the PIs were fully imidized, in which the —NH$_2$ deformation vibration at *ca.* 1623 cm^{-1} assigned to TFMB[36] disappeared, and the C=O asymmetrical stretching vibration at *ca.* 1786 cm^{-1}, symmetrical stretching vibration at *ca.* 1728 cm^{-1} and C—N stretching vibration at *ca.* 1367 cm^{-1} that belong to the imide groups were observed (Fig. S3 in ESI). In our previous work, we also synthesized the diamine monomer 3,3'-(butane-1,4-diylbis(9*H*-carbazole-9,3-diyl))dianiline (DiBu-CzDA)[41] to endow PI-TFMB-6FDA with a rigid-soft structure. Herein, DiBu-CzDA-based PI is employed for comparison in order to investigate the effect of the rigid unit structure on the trade-off between chain rigidity and tight chain packing, in addition to investigating the influence of the ratio of soft units to rigid units.

The dielectric properties at a high frequency of 10 GHz were characterized first, as shown in Figs.1(a), 1(b) and Table 1. The reference PI-TFMB-6FDA showed D_k/D_f ratio of 2.72/0.0075. In contrast, the rigid-soft structure is effective for reducing D_k and D_f at high frequencies, especially for D_f. At the ratio of 5%, the incorporation of DiHe-NaDA led to a slight reduction in D_k/D_f to 2.68/0.007. By further increasing the DiHe-NaDA ratio to 15%, a low D_k/D_f of 2.73/0.005 was

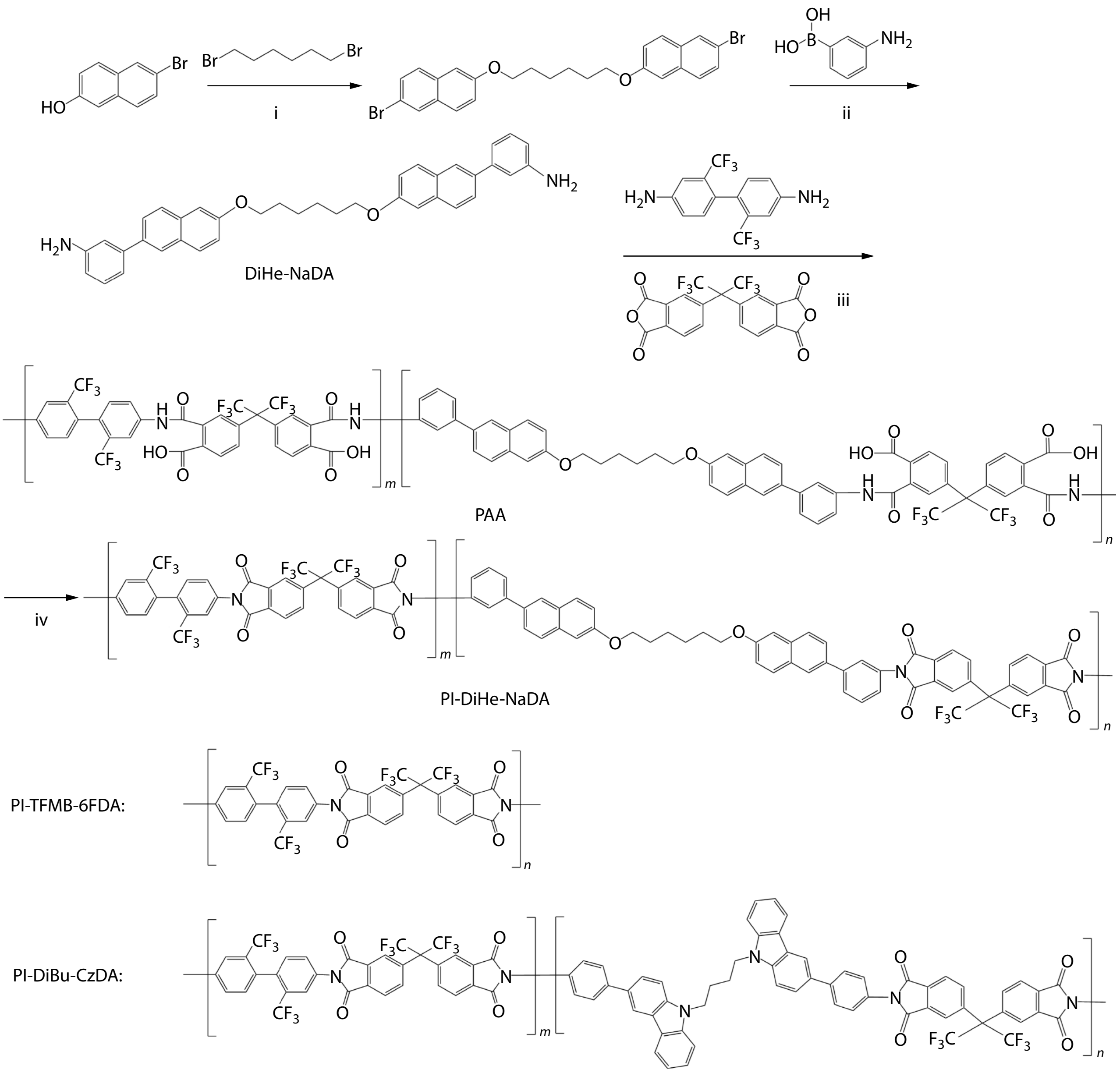

Scheme 1 Synthetic route to PI-DiHe-NaDA: (i) potassium carbonate, and DMF, 85 °C, (ii) Na_2CO_3 aqueous solution (2 mol/L), Pd(dppf)Cl_2, and DMF, 85 °C, (iii) DMAc, room temperature, and (iv) thermal imidization, and the structure of PI-TFMB-6FDA and PI-DiBu-CzDA[41].

achieved. For DiBu-CzDA-based PIs, D_k was all approximately 2.74 at a ratio of 5%–15%. D_f is slightly decreased, but all values are approximately 0.007, regardless of the ratio of DiBu-CzDA.[41] In general, the introduction of an alkyl chain is conducive to lowering the polarizability, which is beneficial for achieving a low D_k/D_f. An increase in the number of alkyl chains should lead to a decrease in the polarizability; thus, D_k/D_f should be further reduced. However, DiBu-CzDA-based PIs preserve D_k/D_f of *ca.* 2.74/0.007, regardless of the ratio of DiBu-CzDA. Thus, DiHe-NaDA-based PIs can achieve a low D_k/D_f at a high ratio of DiHe-NaDA, probably because of other factors such as chain rigidity and packing characteristics.

To gain in-depth insight into these issues, a computer simulation was conducted, as shown in Figs. 1(c)–1(g). Because the low D_k/D_f values of PIs with rigid-soft structures are not entirely related to the introduction of alkyl chains, the chain rigidity and packing characteristics were further studied. The potential energy for the C—N bond adjacent to the imide group was first estimated using the conformers module with a universal force field (Fig. 1f). The larger potential energy difference, which implies a higher energy barrier versus the rotational angle, indicates a higher rigidity of the polymer chains or segments (Fig. 1g). It is found that DiHe-NaDA-TFMB-6FDA possesses higher energy barrier of 172.19 kJ·mol^{-1} than DiBu-CzDA-TFMB-6FDA with energy barrier of 92.22 kJ·mol^{-1}. Obviously, as for the diamines with rigid-soft structure, the rigid unit naphthalene in diamines DiHe-NaDA is able to further restrict the motion of polar imide groups in the glassy state of MPIs, as compared to that of DiBu-CzDA. TFMB-6FDA showed the highest energy barrier of 269.54 kJ·mol^{-1}, probably due to

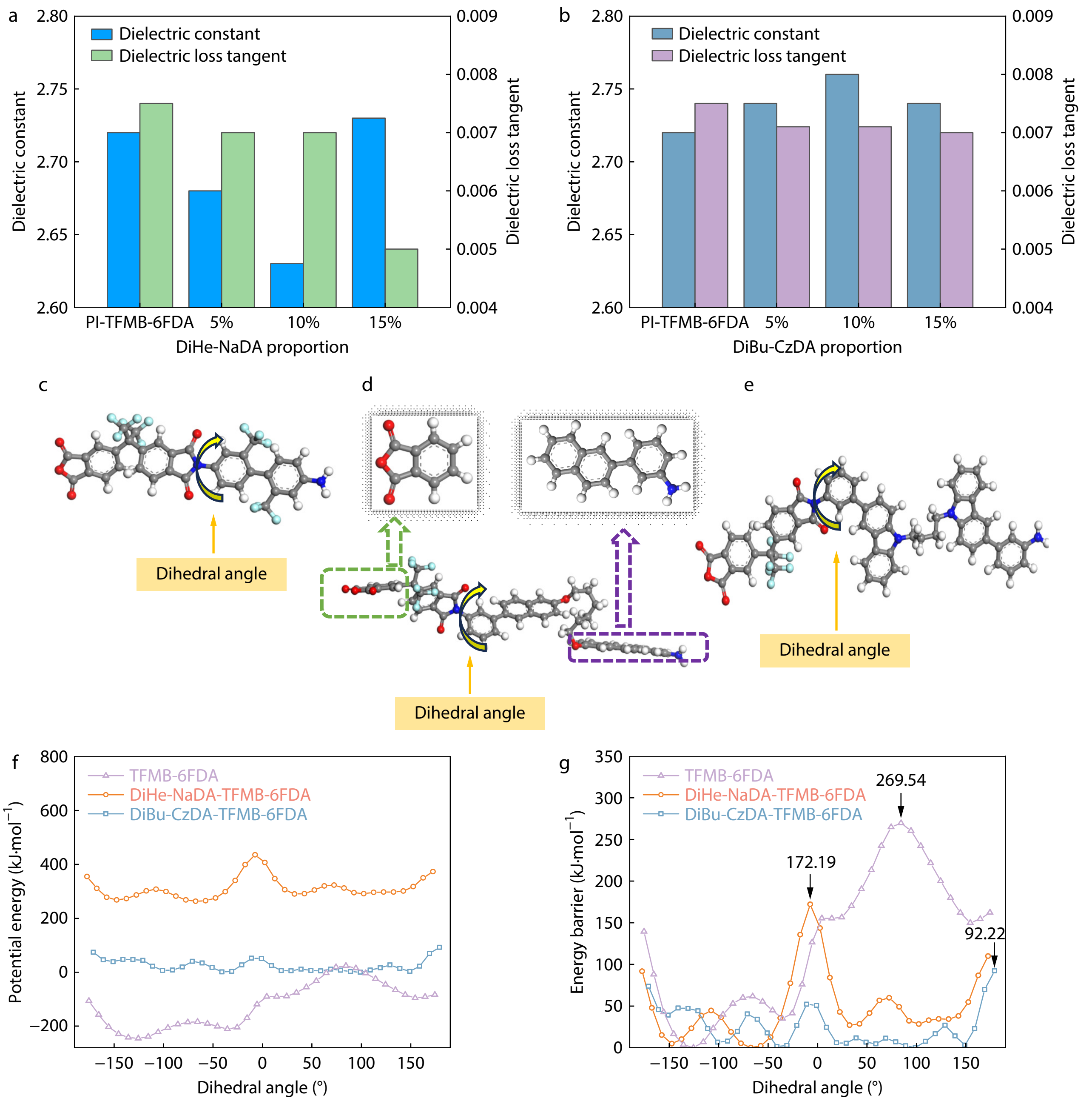

Fig. 1 Dielectric properties of (a) PI-DiHe-NaDA and (b) PI-DiBu-CzDA. Optimized chain conformation of (c) TFMB-6FDA, (d) DiHe-NaDA-TFMB-6FDA and (e) DiBu-CzDA-TFMB-6FDA, and (f) potential energy and (g) energy barrier of the corresponding bond at different dihedral angles.

Table 1 Dielectric properties of MPIs at a frequency of 10 GHz.

MPIs	D_k	D_f
PI-TFMB-6FDA	2.72	0.0075
PI-DiHe-NaDA-5%	2.68	0.0070
PI-DiHe-NaDA-10%	2.63	0.0070
PI-DiHe-NaDA-15%	2.73	0.0050
PI-DiBu-CzDA-5%	2.74	0.0071
PI-DiBu-CzDA-10%	2.76	0.0071
PI-DiBu-CzDA-15%	2.74	0.0070

the presence of the trifluoromethyl side groups.

X-ray diffraction (XRD) measurements were then carried out to investigate the packing nature of polyimides. It was found that the diffraction peak of the resultant poly(amic acid)s at *ca.* 16° was weakened at a low DiHe-NaDA content of 5%–10%, as compared to the reference poly(amic acid) (Fig. 2a). In general, introducing a third monomer can disrupt symmetry, which is not conducive to tight chain packing. However, such a small amount of DiHe-NaDA was insufficient to regulate the packing characteristics of the polymer chains. As the DiHe-NaDA ratio increased to 15%, the packing nature of the resultant poly(amic acid) was similar to that of PI-TFMB-6FDA, indicating that packing characteristics can be regulated by modulating the rigid-soft structure. As a result, PI-DiHe-NaDA-5% and PI-DiHe-NaDA-10% exhibited weakened diffraction

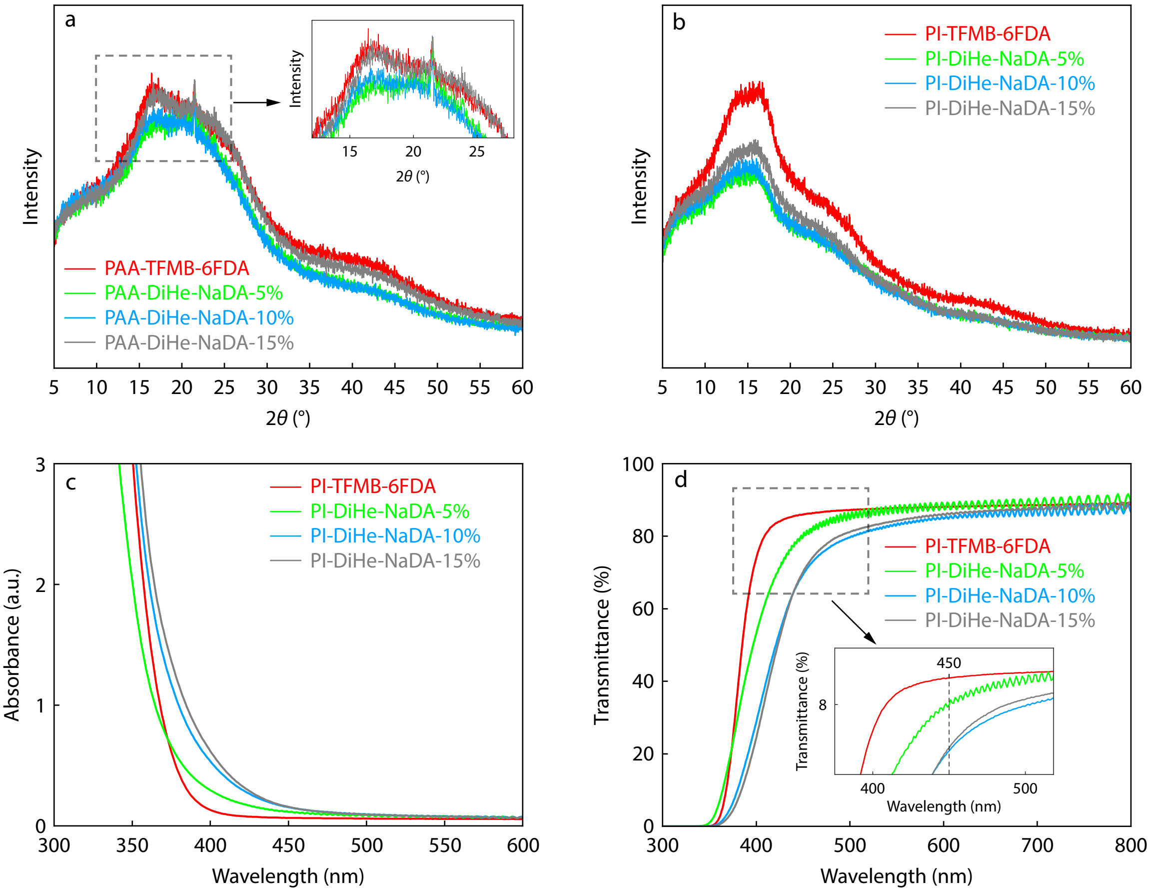

Fig. 2 XRD patterns of (a) poly(amic acid)s and (b) PI films; (c) UV-Vis absorption spectra of PI films; (d) Transmittance spectra of PI films.

peaks at approximately 15.43° and 15.55°, respectively, while the reference PI-TFMB-6FDA showed a diffraction peak at approximately 16.35° (Fig. 2b). With an increase in the DiHe-NaDA ratio to 15%, the diffraction peak was enhanced and further shifted to approximately 15.72°, although it was weaker than that of the reference PI-TFMB-6FDA. This indicated that the incorporation of a lower ratio of DiHe-NaDA resulted in loosened chain packing. However, improving the DiHe-NaDA ratio to 15% enabled the regulation of chain packing, thereby achieving tight chain packing similar to that of the reference PI-TFMB-6FDA. Overall, all the PIs were still amorphous. To further study the packing characteristics of the PIs, UV-Vis transmittance spectra were obtained, as shown in Figs. 2(c) and 2(d). The reference PI-TFMB-6FDA showed an absorption onset of *ca.* 370 nm and $T_{400-800}$ of 93% (normalized transparency based on is the same thickness of 25 μm). In contrast, introducing DiHe-NaDA and DiBu-CzDA effectively enhanced the charge transfer complex (CTC) effect. For instance, at a ratio of 5%, DiHe-NaDA-based PIs exhibited a decreased $T_{400-800}$ of 86%, together with an absorption onset of *ca.* 369 nm. Further increase in the DiHe-NaDA content led to a stronger CTC effect. As the DiHe-NaDA content increased to 15%, the absorption onset was red-shifted to 374 nm, and $T_{400-800}$ was lowered to 80%. This is mainly attributed to the strengthened π-conjugation effect resulting from the naphthalene groups, which is more obvious in the case of DiBu-CzDA-based PIs. At a ratio of 5%, DiBu-CzDA-based PI showed an absorption onset of approximately 374 nm and $T_{400-800}$ of 83%[41]. When the DiBu-CzDA content increased to 15%, the absorption onset was *ca.* 373 nm and $T_{400-800}$ decreased to 68%. Herein, it is also associated with the donor effect of the carbazole moieties in addition to π-π stacking, thereby leading to a stronger CTC effect. Then, the free volume of the PIs is estimated *via* the Forcite module based on a Connolly radius of 0.1 nm (Figs. 3a–3c and Table 2).[42] The incorporation of diamines DiHe-NaDA and DiBu-CzDA yielded a lower fractional free volume (FFV) of 19.69% and 19.56%, respectively, while the reference PI-TFMB-6FDA showed an FFV of 21.06%. The results indicate that PI-DiHe-NaDA-15% and PI-DiBu-CzDA-15% can preserve a higher packing density of the polymer chains than PI-TFMB-6FDA. In addition, the smaller FFVs of PI-DiHe-NaDA-15% and PI- DiBu-CzDA-15% result in a slightly higher D_k.

The mean square displacement (MSD) was explored to study the movability of polymer chains based on the Forcite module[43]. Both DiHe-NaDA-based PI and DiBu-CzDA-based PI exhibited stronger chain mobility than the reference PI-TFMB-6FDA, especially for DiHe-NaDA-based PI, although their main chains incorporated alkyl units (Figs. 3d–3g). As a result, the enhanced mobility of the polymer chains is conducive to achieving closed-chain packing. During the heating process, it is difficult to achieve dense chain packing with PI with a more rigid polymer chain after the partial imidization of poly(amic acid). Therefore, DiHe-NaDA-based PI and DiBu-CzDA-based PI with stronger chain mobility are conducive to

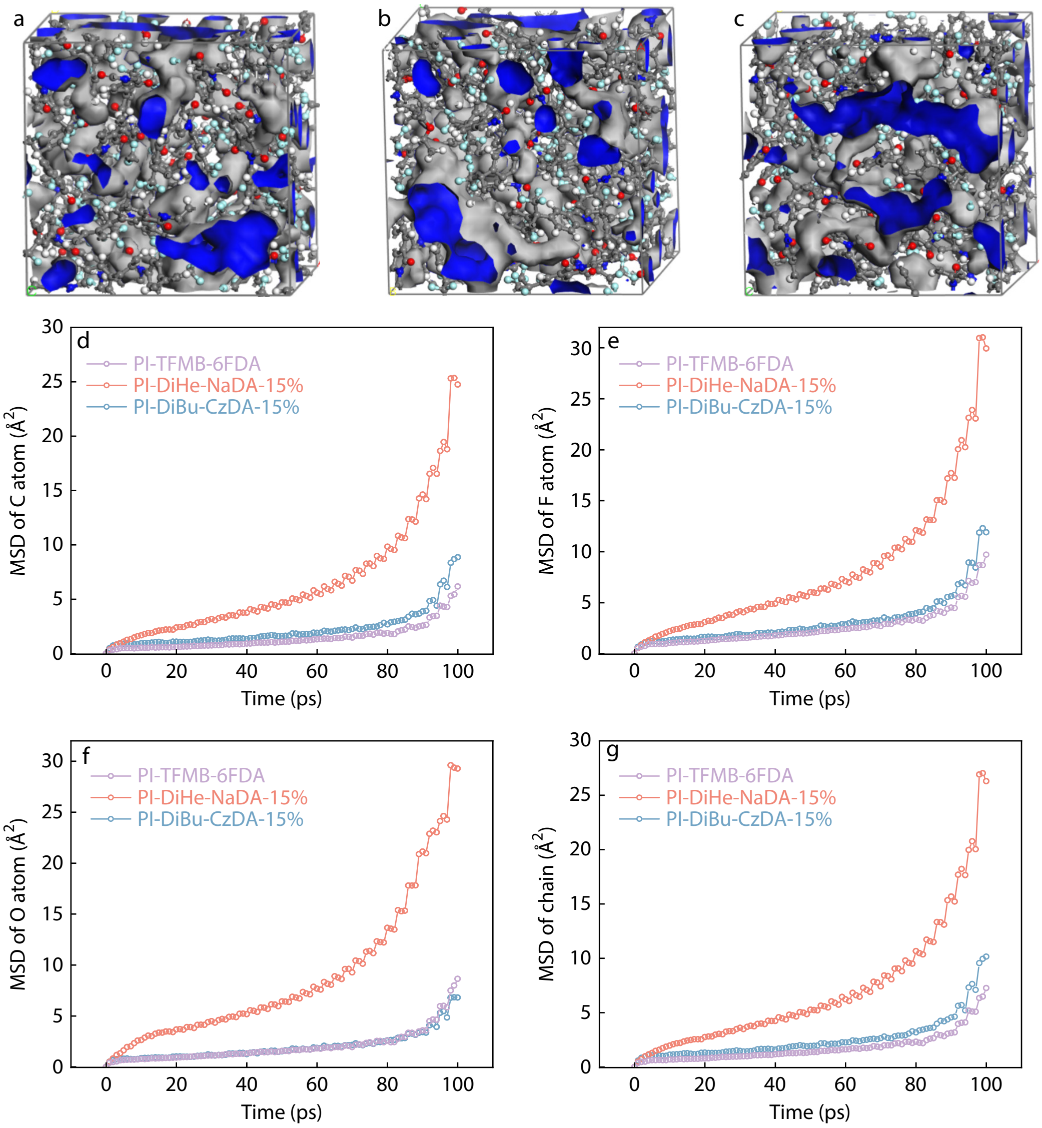

Fig. 3 Simulated free volume image of (a) PI-TFMB-6FDA, (b) PI-DiHe-NaDA-15% and (c) PI-DiBu-CzDA-15% (gray region represents van der Waals surface, and blue region represents Connolly surface). MSD curves of (d) C atom, (e) F atom, (f) O atom and (g) polymer chain of different MPIs.

Table 2 Summary of free volume parameters of MPIs.

MPIs	Total volume (V) (Å^3)	Free volume (V_f) (Å^3)	Fractional free volume (FFV) ^{a} (%)
PI-TFMB-6FDA	15996.53	3368.7	21.06
PI-DiHe-NaDA-15%	17164.05	3379.17	19.69
PI-DiBu-CzDA-15%	17111.75	3347.32	19.56

^{a} FFV is calculated based on the equation: FFV = V_f/V.

forming denser chain packing than the reference PI-TFMB-6FDA, which is mainly attributed to the presence of alkyl chains.

Therefore, dynamic mechanical analysis (DMA) characterization revealed that β-relaxation behavior was effectively confined in DiHe-NaDA-based PIs and DiBu-CzDA-based PIs (Fig. 4b). For instance, the reference PI-TFMB-6FDA shows T_β of *ca*. 270 °C, while the incorporation of DiHe-NaDA leads to a significant decrease in the tanδ value, even at a low DiHe-NaDA content. DiBu-CzDA-based PIs exhibit less β-relaxation behavior only at high DiBu-CzDA contents of more than 10%[41]. In contrast to the reference PI-TFMB-6FDA, the stronger restriction of small-scale molecular motions below T_g in DiHe-NaDA-based PIs and DiBu-CzDA-based PIs is conducive to achieving low D_k/D_f at high frequency. This result is attributed to the denser chain packing and stronger intermolecular interactions originating from the rigid-soft structure. In particular, the rigid naphthalene unit in DiHe-NaDA-based PIs could

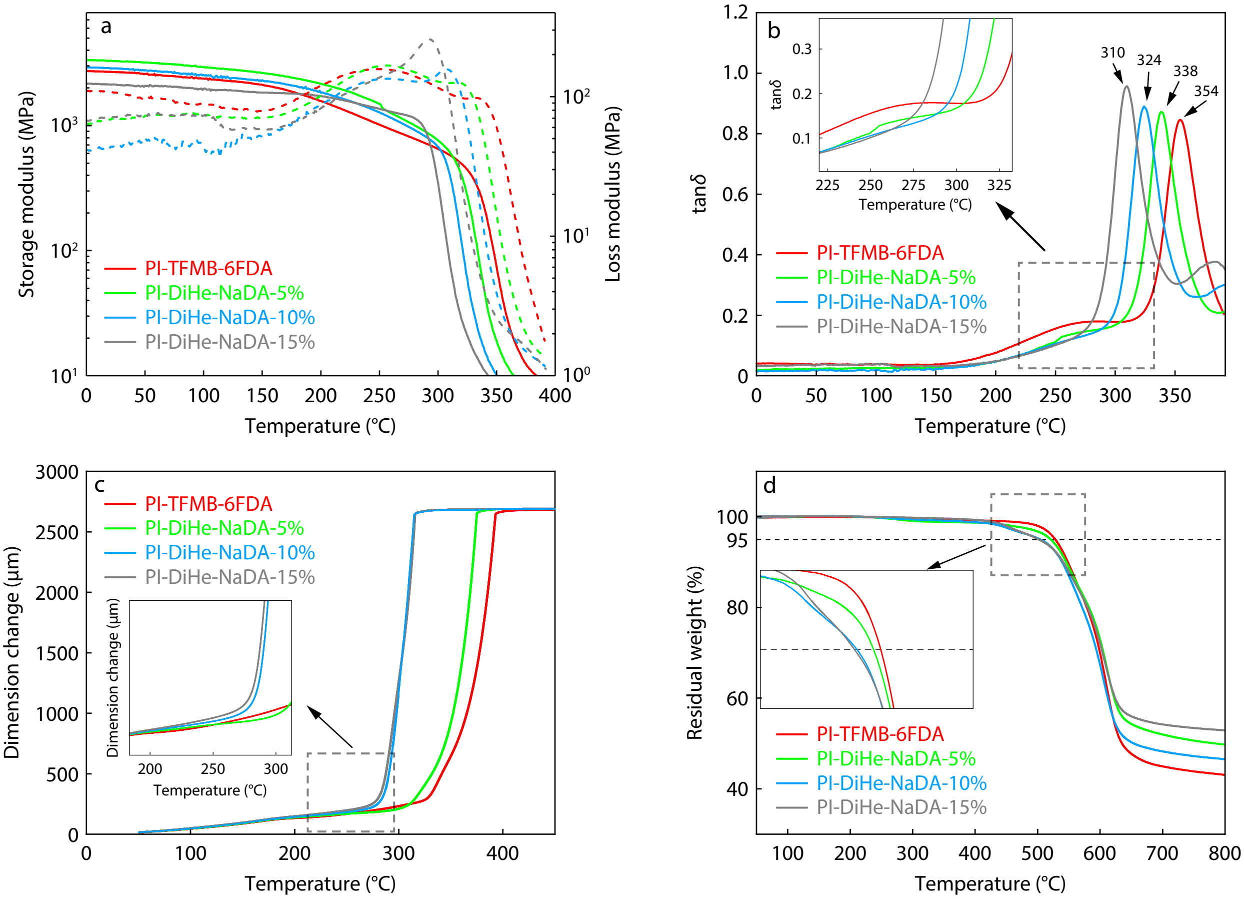

Fig. 4 DMA curves of PI films: (a) storage modulus and loss modulus and (b) tan*δ*. (c) TMA and (d) TGA curves of MPIs.

Table 3 Summary of thermal characteristics, optical properties and mechanical performance of MPIs.

MPIs	T_{d5} (°C)	$T_g{}^a$ (°C)	$T_g{}^b$ (°C)	CTE (ppm/K)	$T_{400-800\ nm}$ (%)	Tensile strength (MPa)	Elongation at break (%)
PI-TFMB-6FDA	528	354	350	50.7	93	115	6.0
PI-DiHe-NaDA-5%	520	338	338	50.3	86	102	4.8
PI-DiHe-NaDA-10%	503	324	289	61.5	80	96	4.7
PI-DiHe-NaDA-15%	501	310	284	62.2	80	105	5.2

[a] T_g was measured by dynamic mechanical analysis (DMA); [b] T_g was measured by thermal mechanical analysis (TMA).

further restrict the motion of polar imide groups as compared to DiHe-NaDA-based PIs, leading to lower D_k/D_f at high frequencies.

However, DMA results revealed that the decline in storage modulus around T_g for DiHe-NaDA-based PIs was significantly more pronounced than that of the reference PI-TFMB-6FDA (Fig. 4a and Table 3). For instance, DiHe-NaDA-based PIs (5%–15%) exhibit increased parameter $(-dE'/dT)_{max}$ of 27.3, 35.3, and 58.8 MPa/°C, respectively, while the reference PI-TFMB-6FDA shows parameter $(-dE'/dT)_{max}$ of 18.5 MPa/°C. This is because of the more flexible chains of the DiHe-NaDA-based PIs. Therefore, the DiHe-NaDA-based PIs (5%–15%) exhibited a lower T_g of 338–284 °C than the reference PI-TFMB-6FDA with a T_g of 350 °C. However, T_g of DiHe-NaDA-based PIs is not low, which is mainly attributed to strong intermolecular interactions and denser chain packing resulting from the rigid-soft structure. It should be noted that the significant decrease in storage modulus around T_g for DiHe-NaDA-based PIs, especially at a ratio of 15%, indicates better thermoplasticity, which is conducive to ensuring PI with favorable processability (Fig. 4a). The thermal mechanical analysis (TMA) results reveal that the incorporation of 5% DiHe-NaDA yields a low coefficient of thermal expansion (CTE) of 50.3 ppm·K^{-1} in the range of 100–250 °C, which is comparable to that of the reference PI-TFMB-6FDA with a CTE of 50.7 ppm·K^{-1} (Fig. 4c and Table 3). As the DiHe-NaDA ratio increased to 10%–15%, the resultant PIs still preserved a favorable CTE of 61.5–62.2 ppm·K^{-1}. In addition, all the DiHe-NaDA-based PIs exhibited high thermal stability, with a weight-loss temperature ($T_{d5\%}$) above 501 °C (Fig. 4d and Table 3).

At lower DiHe-NaDA ratios of 5%–10%, DiHe-NaDA-based PIs exhibit slightly inferior mechanical properties owing to limited intermolecular interactions and looser chain packing (Fig. 5). However, as the DiHe-NaDA content increased to 15%, which is attributed to strong intermolecular interactions and denser chain packing, the DiHe-NaDA-based PI preserved a high tensile strength of 105 MPa and elongation at break of 5.2%, comparable to the reference PI-TFMB-6FDA with a tensile strength of 115 MPa and elongation at break of 6.0%.

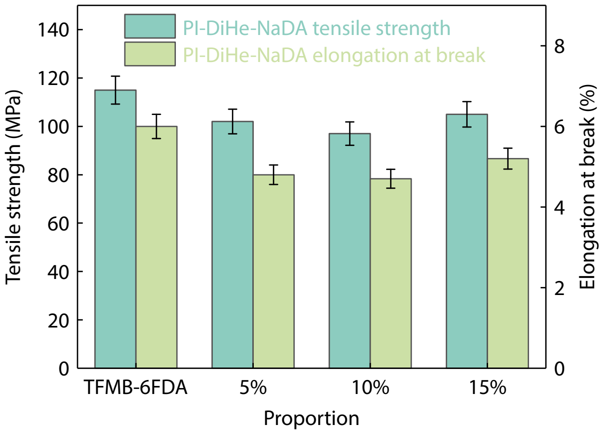

Fig. 5 Mechanical properties of MPIs.

CONCLUSIONS

In conclusion, we developed MPIs with rigid-soft structures based on naphthalene-alkyl-based diamine DiHe-NaDA. This strategy is manifested in two aspects: (1) the soft units can enhance the mobility of polymer chains to endow PI with dense chain packing, and (2) the rigid aromatic units can enhance the intermolecular interaction and further restrict the motion of polar imide groups below T_g. As a result, the as-prepared MPIs can effectively inhibit small-scale molecular motions below T_g, particularly those of the polar imide groups. A low D_k/D_f ratio of 2.73/0.005 was achieved at a high frequency of 10 GHz. In contrast, the reference PI-TFMB-6FDA exhibited D_k/D_f of 2.72/0.0075. Furthermore, PIs with rigid-soft structures exhibit good chain flexibility above T_g and thereby, good thermoplasticity. Simultaneously, the DiHe-NaDA-based PIs were able to preserve favorable thermal stability. This strategy provides a new guide for the development of MPIs with a low D_k/D_f for high-frequency communication applications.

Conflict of Interests

The authors declare no interest conflict.

Electronic Supplementary Information

Electronic supplementary information (ESI) is available free of charge in the online version of this article at http://doi.org/10.1007/s10118-025-3338-2.

Data Availability Statement

The data supporting the findings of this study are available from the corresponding author upon reasonable request.

ACKNOWLEDGMENTS

This work was financially supported by the National Natural Science Foundation of China (Nos. U20A20340 and 52001068), Key-Area Research and Development Program of Guangdong Province (No. 2020B010182001), Dongguan Key Research & Development Program (No. 20231200300192), Science and Technology Projects in Guangzhou (No. 2025A04J3832), Foshan Introducing Innovative and Entrepreneurial Teams (No. 1920001000108), and Guangzhou Hongmian Project (No. HMJH-2020-0012) .

REFERENCES

1 Zhang, C.; He, X.; Lu, Q. High-frequency low-dielectric-loss in linear-backbone-structured polyimides with ester groups and ether bonds. *Commun. Mater.* **2024**, *5*, 1−11.

2 Qin, Y.; Yin, Q.; Lyu, J.; Wang, X.; Liu, X. Tuning the persistence lengths of main chain towards colorless and transparent polyimide with low dielectric loss and excellent general properties. *Polymer* **2024**, *298*, 126853.

3 Li, H.; Wei, P.; Wang, Y.; Zhu, Q.; Wang, X.; Gao, W.; Tao, L.; Ma, K.; Hu, Z.; Chen, W. High-frequency 5G substrate: Low dielectric biphenyl polyimide with low CTE and high thermal stability. *Mater. Today Adv.* **2024**, *23*, 100514.

4 Zhang, C.; He, X.; Lu, Q. Polyimide films with ultralow dielectric loss for 5G applications: Influence and mechanism of ester groups in molecular chains. *Eur. Polym. J.* **2023**, *200*, 112544.

5 Peng, Z.; Ye, A.; Zhang, L.; Li, X.; Lian, C.; Li, C. Micro-crosslinked polyimide nanocomposites with low dielectric constant and low dielectric loss for microwave antenna with molecular dynamics. *Compos. Commun.* **2024**, *46*, 101804.

6 Li, H.; Bao, F.; Li, S.; Li, Y.; Li, X.; Mu, K.; Wang, M.; Zhu, C.; Xu, J. Preparation of fluorinated polyimides with low dielectric constants and low dielectric losses by combining ester groups and triphenyl pyridine structures. *Polym. Chem.* **2024**, *15*, 22−29.

7 Qu, C.; Shan, L.; Zhang, G.; Sun, R. Preparation and dielectric properties research of a novel kind of intrinsic silane-containing polyimide. *Polymer* **2023**, *285*, 126361.

8 Nagella, S. R.; Park, S. S.; Chitumalla, R. K.; Jang, J.; Ha, C. S. Intrinsic low-dielectric-constant polyimides based on a novel diamine having $-CF_3$ groups and kinkable 1,4-diisopropylbenzene units. *Polymer. Int.* **2023**, *73* (3), 238−247.

9 Li, K.; Yang, L.; Yang, L.; He, L.; Du, J.; Li, X. Low dielectric polyimide microsphere/polyimide composite films based on porous polyimide microsphere. *Polym. Eng. Sci.* **2024**, *64*, 5166−5175.

10 Sun, W.; Yang, M.; Peng, K.; Fu, Y. All-organic hyper-crosslinked polymer/polyimide composite films with ultralow high-frequency dielectric constant. *Macromol. Rapid Commun.* **2023**, *44*, 2200956.

11 Li, Y.; Ma, B.; Zhang, R.; Luo, X. Mechanically strong, thermal-insulated, and ultralow dielectric polyimide aerogels with adjustable crosslinking methods. *Polymer* **2022**, *253*, 125035.

12 Kim, S.; Son, J.; Park, H.; Jeong, E.; Nam, K. H.; Bae, J. S. Polymer concentration and liquid-liquid demixing time correlation with porous structure of low dielectric polyimide in diffusion-driven phase separation. *Polymers* **2022**, *14*, 1425.

13 Zhang, P.; Zhang, L.; Zhang, K.; Zhao, J.; Li, Y. Preparation of polyimide films with ultra-low dielectric constant by phase inversion. *Crystals* **2021**, *11*, 1383.

14 Kourakata, Y.; Onodera, T.; Kasai, H.; Jinnai, H.; Oikawa, H. Ultra-low dielectric properties of porous polyimide thin films fabricated by using the two kinds of templates with different

particle sizes. *Polymer* **2021**, *212*, 123115.

15 Zou, B. Y.; Qiu, L. H.; Lei, H. Y.; Liu, J. M.; Peng, W. F.; Zhao, H. Q.; Bao, F.; Huang, M. J. Fluorinated colorless polyimides with high heat-resistance and low birefringence. *Chinese J. Polym. Sci.* **2023**, *41*, 1599−1608.

16 Fan, H.; Xie, T.; Wang, C.; Zhang, Y.; Pan, S.; Li, J.; Zhang, Y.; Guan, S.; Yao, H. Low-dielectric polyimide constructed by integrated strategy containing main-chain and crosslinking network engineering. *Polymer* **2023**, *279*, 126035.

17 Peng, W.; Lei, H.; Qiu, L.; Bao, F.; Huang, M. Perfluorocyclobutyl-containing transparent polyimides with low dielectric constant and low dielectric loss. *Polym. Chem.* **2022**, *13*, 3949−3955.

18 He, X.; Zhang, S.; Zhou, Y.; Zheng, F.; Lu, Q. The “fluorine impact” on dielectric constant of polyimides: a molecular simulation study. *Polymer* **2022**, *254*, 125073.

19 Wu, X.; Cai, J.; Cheng, Y. Synthesis and characterization of high fluorine-containing polyimides with low-dielectric constant. *J. Appl. Polym. Sci.* **2021**, *139*, 51972.

20 Tao, L.; Yang, H.; Liu, J.; Fan, L.; Yang, S. Synthesis and characterization of highly optical transparent and low dielectric constant fluorinated polyimides. *Polymer* **2009**, *50*, 6009−6018.

21 Sawada, R.; Ando, S. Polarization analysis and humidity dependence of dielectric properties of aromatic and semialicyclic polyimides measured at 10 GHz. *J. Phys. Chem. C* **2024**, *128*, 6979−6990.

22 He, J.; Wu, X.; Cheng, Y. Low dielectric post-cured benzocyclobutene-functionalized fluorine-containing polyimide material. *Eur. Polym. J.* **2023**, *196*, 112334.

23 Bei, R.; Qian, C.; Zhang, Y.; Chi, Z.; Liu, S.; Chen, X.; Xu, J.; Aldred, M. P. Intrinsic low dielectric constant polyimides: relationship between molecular structure and dielectric properties. *J. Mater. Chem. C* **2017**, *5*, 12807−12815.

24 Li, H.; Lan, X.; Bao, F.; Li, S.; Zhu, H.; Zhu, Z.; Li, Y.; Wang, M.; Zhu, C.; Xu, J. Preparation of triphenylamine polyimides with low dielectric constants with different side group sizes based on β-relaxation theory. *Eur. Polym. J.* **2024**, *211*, 112969.

25 Jiang, S.; Zhou, Z.; Zhang, J.; Yi, N.; Wang, J.; Zhao, J.; Fan, L.; Wu, Y.; Gan, F. Fabrication of high-performance polyimide films by tailoring coordination bond and chain rigidity. *Eur. Polym. J.* **2024**, *214*, 113161.

26 Chen, Y.; Chen, X.; Wang, Y.; Nie, Z.; Wang, X.; Tan, J.; Zhuang, Y.; Liu, X.; Wang, X. Increasing twist rigidity to prepare polyimides with low dielectric constants and dissipation factors over a wide temperature range. *Macromolecules* **2023**, *56*, 9379−9388.

27 Qin, Y.; Yin, Q.; Lyu, J.; Wang, X.; Liu, X. Preparation of polyimide films with ultralow dielectric loss at high frequency by reducing intermolecular friction. *Polymer* **2024**, *309*, 127432.

28 Meng, X.; Wen, Y.; Wang, X.; Shen, D.; Yan, J.; Wang, Z. High performance imide oligomers and thermosets derived from 9,9-bis(3,4-dicarboxyphenyl)fluorene dianhydride. *Polymer* **2023**, *281*, 126086.

29 Cheng, Y. C.; Chen, Y. C.; Lin, Y. C.; Kuo, C. C.; Chen, W. C. Exploring the cross-linking effect on decreasing the dielectric constant and dissipation factor of poly(ester imide)s at a high frequency of 10−40 GHz. *ACS Appl. Polym. Mater.* **2023**, *5*, 7907−7917.

30 Lee, J. S.; Yan, Y. Z.; Park, S. S.; Ahn, S. K.; Ha, C. S. A novel diamine containing ester and diphenylethane groups for colorless polyimide with a low dielectric constant and low water absorption. *Polymers* **2022**, *14*, 4504.

31 Zhu, T.; Yu, Q.; Zheng, W.; Bei, R.; Wang, W.; Wu, M.; Liu, S.; Chi, Z.; Zhang, Y.; Xu, J. Intrinsic high-k–low-loss dielectric polyimides containing ortho-position aromatic nitrile moieties: reconsideration on Clausius–Mossotti equation. *Polym. Chem.* **2021**, *12*, 2481−2489.

32 Zhou, Y.; Zhang, S.; Zheng, F.; Lu, Q. Intrinsically black polyimide with retained insulation and thermal properties: a black anthraquinone derivative capable of linear copolymerization. *Macromolecules* **2021**, *54*, 9307−9318.

33 Han, S.; Li, Y.; Hao, F.; Zhou, H.; Qi, S.; Tian, G.; Wu, D. Ultra-low dielectric constant polyimides: combined efforts of fluorination and micro-branched crosslink structure. *Eur. Polym. J.* **2021**, *143*, 110206.

34 Xiao, H.; Huang, J.; Wang, M.; Huang, W.; Li, M.; Jin, G. Unraveling molecular loss processes for dielectric polymers in the Terahertz frequency range: impact of polarity and chain rigidity. *Polymer* **2024**, *297*, 126855.

35 Jian, L. F.; Lu, Z. Y.; Zhang, J. Y.; Yuan, H. B.; Zhang, H.; Ge, H.; Tan, W. Y.; Cui, T. T.; Min, Y. G. Thermoplastic polyimide with low dielectric properties enabled by the 2,2′-spirobifluorene group. *J. Appl. Polym. Sci.* **2024**, *141*, 55686.

36 Tan, W. Y.; Jian, L. F.; Chen, W. P.; Zhang, Y. W.; Lu, X. C.; Huang, W. J.; Zhang, J. S.; Wu, J. W.; Feng, J. L.; Liu, Y. D.; et al. A facile strategy for intrinsic low-D_k and low-D_f polyimides enabled by spirobifluorene groups. *Chinese J. Polym. Sci.* **2022**, *41*, 288−296.

37 Zhang, L.; Liu, J.; Luo, L.; Liu, X.; Wang, X. All-organic polyimide/Cl-HBC composite film with high breakdown strength and ultra-low dielectric loss. *Polymer* **2022**, *245*, 124702.

38 Kim, S.; Lee, Y.; Park, J.; So, Y.; Jung, H. T.; Ko, M. J.; Won, J. C.; Jeong, S.; Kim, Y. H. Green and facile synthesis of hybrid composites with ultralow dielectric properties from water-soluble polyimide and dual-porous silica nanoparticles. *ACS Appl. Mater. Interfaces* **2022**, *15*, 4408−4418.

39 Li, X. T.; Zhu, X. M.; Dong, J.; Zhao, X.; Zhang, Q. H. Preparation of low-dielectric permittivity polyimide resins with high surface activity from chemically bonded hyperbranched polysiloxane. *Chinese J. Polym. Sci.* **2021**, *39*, 1200−1210.

40 Zhao, G.; Mu, X.; Ma, D.; Wang, S.; Pan, J.; Cui, J.; Qi, M. Dielectric and mechanical properties of TiO_2/polyimide composites with low dielectric constant. *Polym. Eng. Sci.* **2023**, *63*, 1953−1960.

41 Lu, Z.; Jian, L. F.; Zhang, J.; Du, Q.; Yuan, Z.; Tan, W.; Min, Y. Intrinsically microporous polyimides based on a rigid–soft structure for hydrogen separation. *ACS Appl. Mater. Interfaces* **2025**, *17*, 9786−9796.

42 Park, C. H.; Tocci, E.; Kim, S.; Kumar, A.; Lee, Y. M.; Drioli, E. A simulation study on OH-containing polyimide (HPI) and thermally rearranged polybenzoxazoles (TR-PBO): relationship between gas transport properties and free volume morphology. *J. Phys. Chem. B* **2014**, *118*, 2746−2757.

43 Rahmati, M.; Modarress, H.; Gooya, R. Molecular simulation study of polyurethane membranes. *Polymer* **2012**, *53*, 1939−1950.